Paper 1

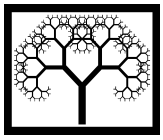

Proceedings of the Eleventh International Conference
on Computational Structures Technology,
B.H.V. Topping, (Editor),
Civil-Comp Press, Stirlingshire, Scotland

The Influence of Residual Stresses on the Buckling Behaviour of Rack Uprights

M.M. Pastor, J. Bonada, F. Roure and M. Casafont
Department of Strength of Materials and Structural Engineering
Escola Tècnica Superior d'Enginyeria Industrial de Barcelona (ETSEIB)
Universitat Politècnica de Catalunya (UPC), Barcelona, Spain

Abstract

The first step of this investigation has been to analyze the cold roll forming process of the upright, using a specific finite element (FE) program that includes geometric and material non-linearity. After the process simulation, the residual strains and stresses are obtained. In a second step, these values are introduced as initial stress state in the FE model that will be used to analyse the behaviour of the upright column under compression. The compression analysis is also completed with geometric and material non linearity, so that elastic and inelastic buckling can be modelled, and the ultimate loads are obtained. The results are compared with the ones obtained by the classic two step method (linear elastic buckling to obtain an initial deformation shape and then use it as initial geometric imperfection for the nonlinear analysis). They are also compared to the results obtained experimentally.

Keywords: buckling, cold-formed sections, residual stresses, finite element analysis.

1 Introduction

The buckling behaviour of rack uprights subject to compression is influenced by many different factors (length of the column, end section boundary conditions, geometric imperfections, presence of perforations, etc.). For the uprights obtained by cold roll forming, the changes introduced in the material by this process (residual stresses and strain hardening) have also an important effect.

For numerical prediction of the ultimate strength of cold-formed steel thin-walled sections in compression [1], a finite element model including geometric and material nonlinearities is commonly used. The standard approach consists of modelling imperfection distribution as buckling modes (linear buckling analysis). Generally the first (critical) buckling mode is selected for use in subsequent nonlinear analysis. As for imperfection magnitudes, values from standards and literature are

usually taken. These values include the effects of residual stresses from the cold roll forming process and other factors such as loading eccentricity, etc. Therefore, both distribution and magnitude are more a modelling convenience than a physical reality. The column's initial imperfections can also be included as different linear combinations of the critical buckling mode shapes obtained through preliminary linear stability analysis [2]. Statistical information on local and distortional buckling imperfection magnitudes that were measured on actual cross-sections is provided in [3]. This paper shows values with 25%, 50% and 75% of probability of exceedance for both types of imperfections. Schafer's research group is involved with continuing this imperfection spectrum work [1]. On the other hand, many researchers have used measured geometric imperfections to study their effect on the ultimate strength of cold-formed steel members [3, 4]. A mechanistic model for prediction of residual stresses and strains is provided in [5], which allows the modeller to consider their effects by generating a more accurate set of initial conditions.

In the present work the cold roll forming process has been simulated and residual strains and stresses numerically derived by means of finite element modelling of cold work of steel sheet including geometric and material non linearity. The attention is focused on the influence of the residual stresses in the buckling behaviour of uprights with open thin-walled steel sections.

The aim of the present investigation is to compare the results obtained from nonlinear analysis including residual stresses as an initial stress state, with those provided by the classic two step method (linear elastic buckling to obtain an initial deformation shape and then use it as initial geometric imperfection for the nonlinear analysis). They are also compared to the results from experimental testing.

2 Obtaining residual stresses

The steel sheet forming is reproduced through COPRA [6] and the parameters involved in the analysis are checked until the formed profile is approved. Once the geometry has been properly adjusted, the finite element model provides comprehensive information of the stresses, strains and displacements introduced in the profile by the cold roll forming process.

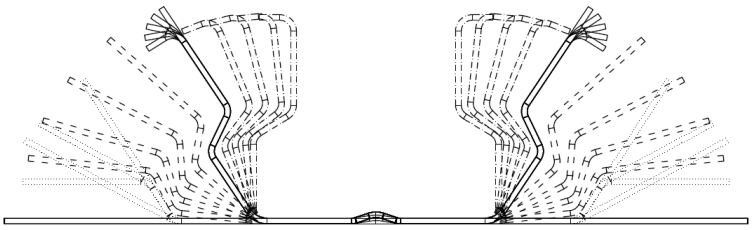

Figure 1: Flower pattern with 20 forming stands

The flower pattern is designed by means of twenty forming line stations (Figure 1) by using the deformation technology module, which acts as a pre-processor of the non-linear finite element analysis module (Figure 2). The Swift's curve is used to define the material plastic behaviour.

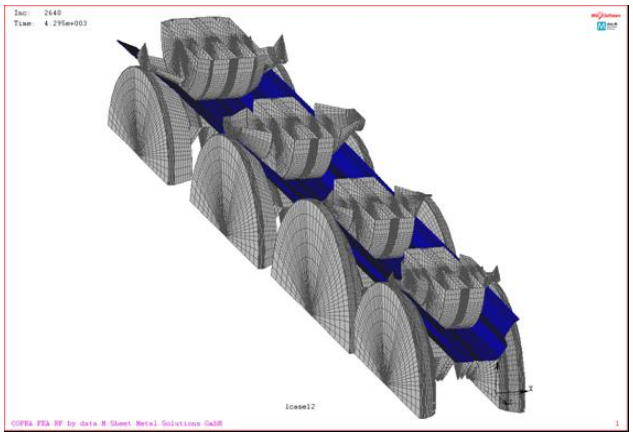

Figure 2: Simulated roll forming stages

Through these simulations it is possible to analyse the changes undergone by the steel sheet, from its initial state until leaving the production line with the desired shape. The large strains introduced in the process, beyond the yield point, make several areas to deform plastically, which generates important residual strains and stresses.

Figure 3 shows the values of equivalent plastic strains reached during the roll forming process at the midsection of the roll forming profile. As seen, the highest values belong to the corner regions.

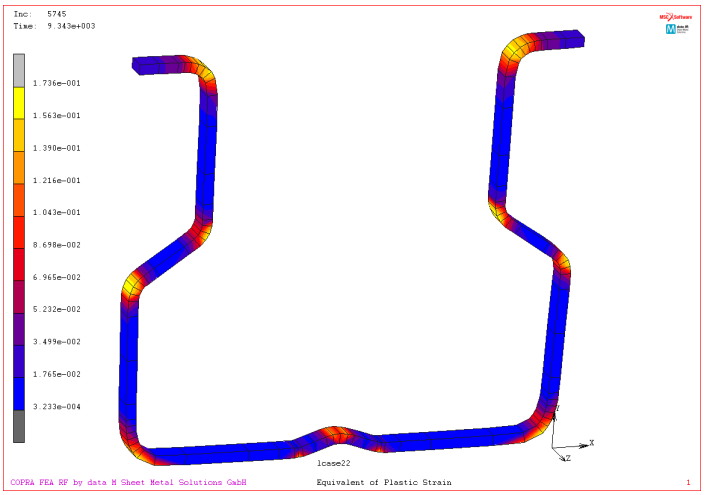

Figure 3: Equivalent plastic strain distribution

The transverse and longitudinal residual strains caused by the rolling operation are plotted in Figures 4-5 at the midsection of the formed profile. The node at the outer end of the lip is defined by the coordinate $S = 0$ and the highest value of S ($S = 120$) belongs to the centre of the section (symmetry plane of the cross-section).

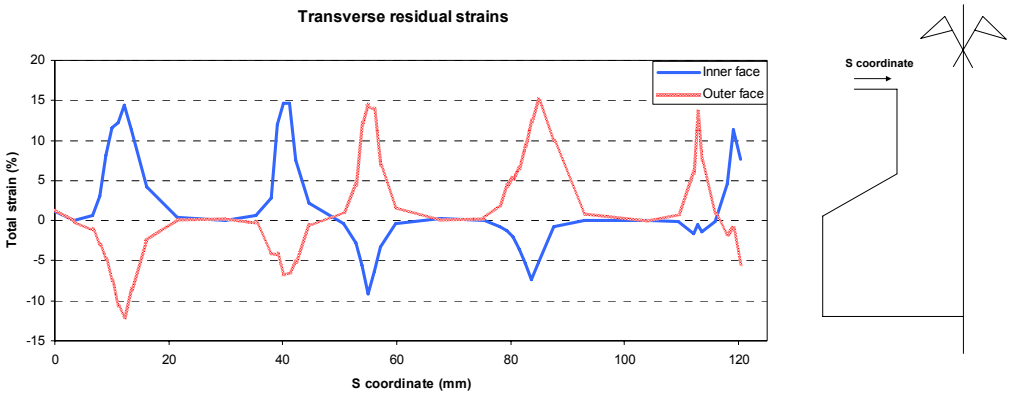

Figure 4: Transverse residual strains over half cross-section

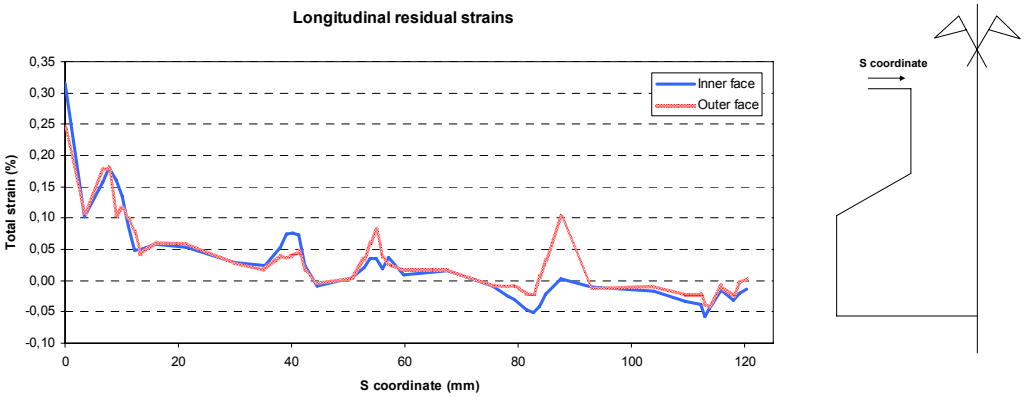

Figure 5: Longitudinal residual strains over half cross-section

3 Nonlinear analysis modelling residual stresses

3.1 Transferring

The FE model for nonlinear analysis of upright in compression has been created using ANSYS 13.0 [7]. The residual strains of a section of the formed profile are selected from COPRA simulation and introduced in the ANSYS finite element model. The section is located at the central portion of the profile to prevent local effects and ensure a representative residual stress distribution. This residual strain pattern is spread out along the whole profile. The values are taken at the integration points.

The transfer of residual strains from COPRA to ANSYS is done. The residual strain pattern is extended along the column. Then, the member is fixed at both ends (all DOF constrained, to prevent distortion) representing the clamped condition and axial symmetry along the Z axis is applied. These boundary conditions, shown in Figure 8, reproduce the experimental set-up, as seen in Figure 12.

3.2 Post equilibrium

After equilibrium of residual strains, the initial elastic strains (from roll forming process, Figures 4-5) and the final elastic strain (once transferred and after equilibrium) are compared in Figures 6-7. As it can be seen, they are very similar on both faces of cross-section. This demonstrates that data transfer from COPRA to ANSYS works correctly because the same residual strain pattern is obtained.

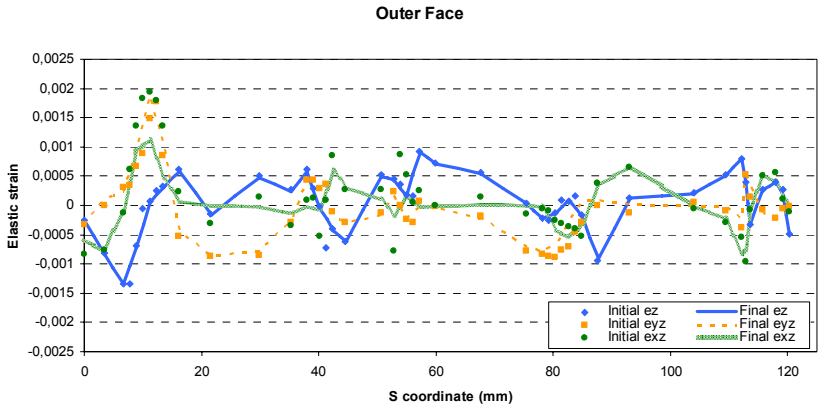

Figure 6: Elastic strains in the outer face
Initial: from roll forming. Final: after transferring and equilibrium

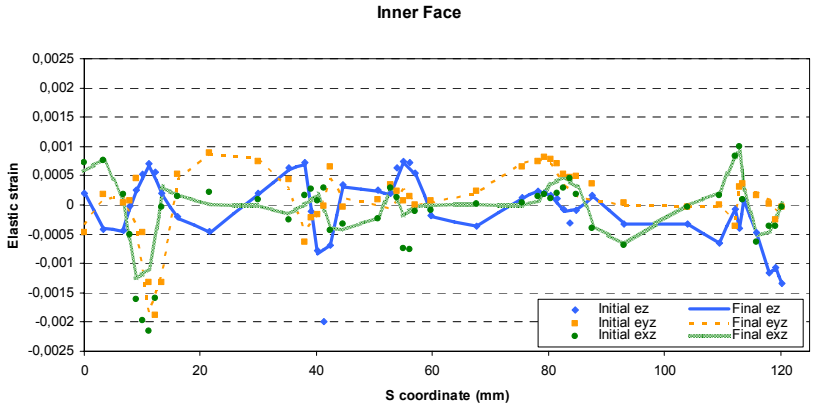

Figure 7: Elastic strains in the inner face
Initial: from roll forming. Final: after transferring and equilibrium

After equilibrium analysis, the column exhibits a deformed shape due to the action of residual strains introduced. This artificial geometrical imperfection is really

small if compared to those used in conventional models: 1.8 mm as [3], and 1.38 mm as [8]. It should be kept in mind that those include not only residual stresses, but also geometrical imperfection, load eccentricity, etc. For a 1000 mm column length, the total displacement field is shown in Figure 8, where it can be seen that the maximum values (0.348348 mm) belong to the central portion of the member.

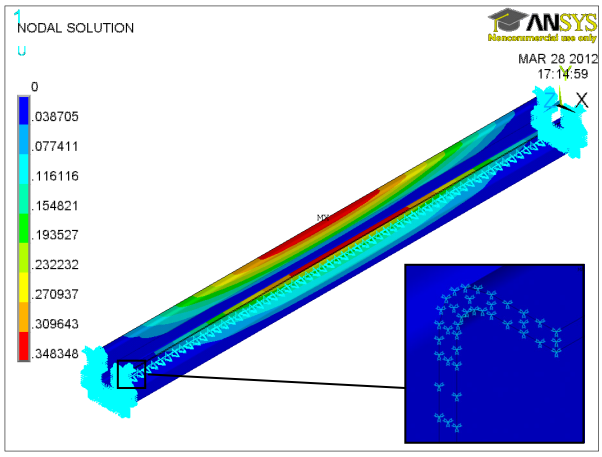

Figure 8: Boundary conditions and deformed shape

3.3 Residual stress distribution

Longitudinal (SZ) residual stress distributions are plotted on both faces over cross-section in Figures 9-11. Figure 9 shows distribution on the inner face, Figure 10 shows distribution on the outer face and Figure 11 shows membrane stress distribution. Longitudinal residual stresses vary trough the thickness, given that a different distribution (in sign and magnitude) is derived on both the inner and outer face of the cross-section. As observed, the highest longitudinal stress values are around the corners.

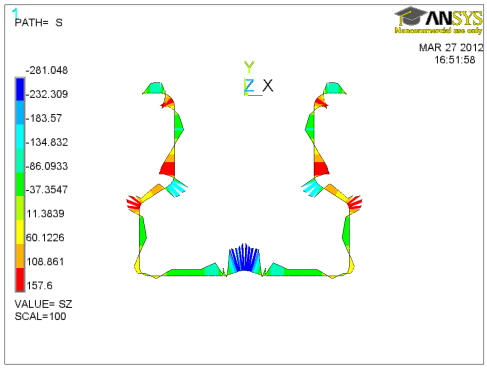

Integration point values

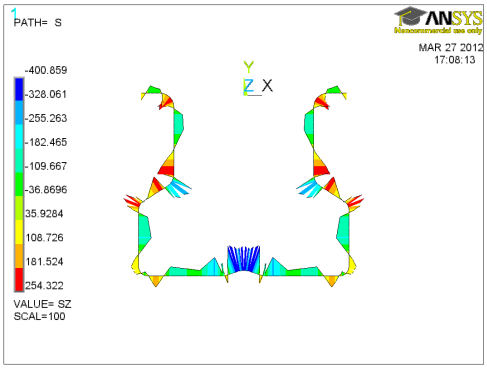

Extrapolation to the nodes

Figure 9: Longitudinal residual stress distribution on the inner face

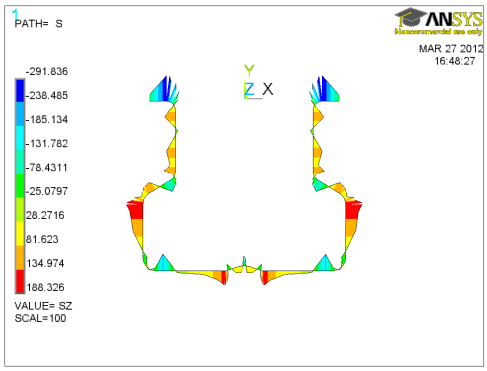

Integration point values

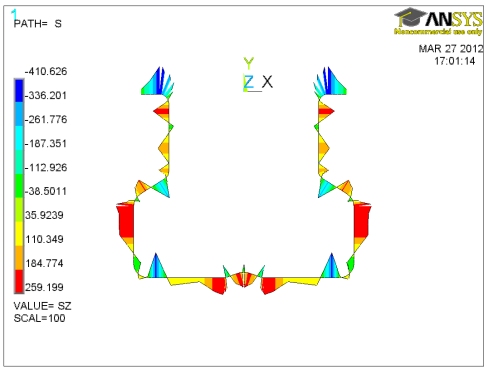

Extrapolation to the nodes

Figure 10: Longitudinal residual stress distribution on the outer face

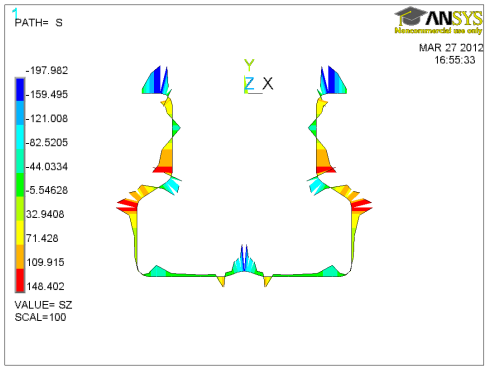

Integration point values

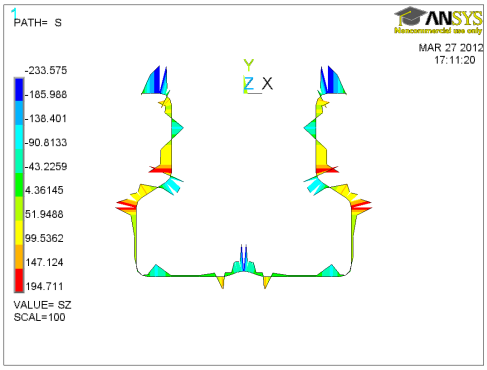

Extrapolation to the nodes

Figure 11: Longitudinal residual stress distribution on the membrane

Integration point values and extrapolation to the nodes are both presented. Special attention must to be paid to graphs presenting values calculated by extrapolation to the nodes. Correct values belong to integration points. However, extrapolated values have been used to compare FE results to strain gauge measurements, since readings are taken on material surface.

4 Comparison of results

In this Section results obtained by nonlinear finite element analysis - both the standard approach (without residual stresses) and model including residual stresses - are compared with the experimental tests carried out by the authors. Seven different column lengths ranging from 250 to 1500 mm tested in compression have been analyzed.

4.1 Experimental tests

Plates are clamped to the end section and restrain the local distortion of the section as shown in Figure 12. The details of such testing are spelled out in [9, 10]. Table 1 shows the experimental results for all tested lengths.

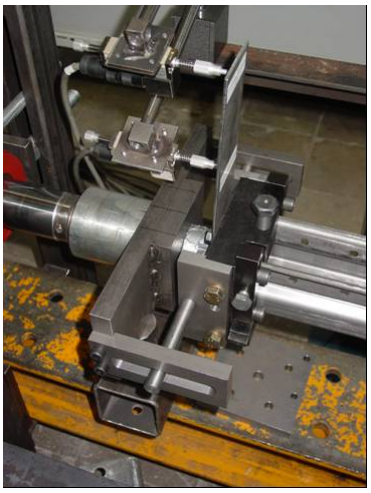

Figure 12: Experimental boundary conditions at ends of upright

Column length (mm)	Ultimate load (N)			
	Spec1	Spec2	Spec3	Mean
250	177522	178846	176786	177718
400	157921	156283	157097	157100
600	138547	139145	138321	138671
800	132111	133063	129776	131650
1000	125277	130287	132641	129402
1200	121202	129158	132052	127471
1500	121879	111334	101534	111582
1800	93578	92449	95363	93797
2200	64079	65021	64285	64462
2600	48903	50041	49295	49413

Table 1: Experimental results

4.2 Standard approach. Conventional model

Experimental test features have been reproduced in the finite element model, in particular boundary conditions (Figure 12-13). The material has been modelled as in Section 2. Shell181 (4-node finite strain shell element) has been used. The compression analysis is done with geometric and material non linearity, so that elastic and inelastic buckling can be modelled, and ultimate loads are obtained.

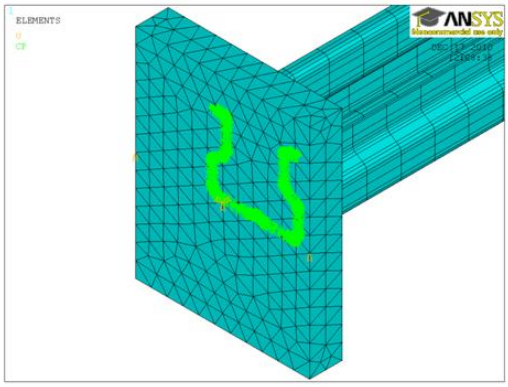

Figure 13: Numerical boundary conditions at ends of upright

This is the classic two step method: linear elastic buckling to obtain an initial deformation shape and then use it as initial geometric imperfection shape for the nonlinear analysis. Further details can be found in [9].

4.2.1 Using critical buckling mode

The first (critical) buckling mode is selected from linear analysis for use in subsequent nonlinear analysis.

The second column in Table 2 shows the numerical results. Imperfection sizes used are shown in the third column. The fourth column presents the ratio numerical/experimental ultimate load, and buckling mode is given in the last column.

Column length (mm)	Ultimate load (N)	Imperfection size (mm)		FEM/EXP	Buckling mode
250	174446	Web/200	0.403	0.98	1 local/distortional
400	172650	Web/200	0.403	1.10	1 local/distortional
600	142792	Flange/50	1.38	1.03	1 distortional (in)
800	153455	Flange/50	1.38	1.16	1 distort (asym)
1000	149781	Flange/50	1.38	1.15	1 distort (asym)
1200	142419	Flange/50	1.38	1.10	1 distort (asym)
1500	124813	Length/1000	1.5	1.12	1 global (flex-tors)
			Mean	1.09	
			S	0.064	

Table 2: FEM results using the critical mode

As seen in Table 2, this common procedure overestimates the carrying load capacity of the upright for lengths prone to distortional failure.

4.2.2 Using appropriate buckling mode

Consecutive buckling modes from linear analysis are checked until obtaining the lowest ultimate load. Analysis is done under the same conditions as previous Section.

Column length (mm)	Ultimate load (N)	Imperfection size (mm)		FEM/EXP	Buckling mode
250	172217	Web/200	0.403	0.97	1
400	166072	Web/200	0.403	1.06	5
600	142545	Flange/50	1.38	1.08	1
800	129515	Flange/50	1.38	0.98	3
1000	123831	Flange/50	1.38	0.95	2
1200	120668	Flange/50	1.38	0.93	2
1500	110567	Length/1000	1.5	0.99	4
			Mean	0.99	
			S	0.054	

Table 3: FEM results using the appropriate mode

Figure 14 compares the numerical results according to 4.2.1 and 4.2.2 with the experimental values. The graph shows ultimate load versus column length. The three blue points represent experimental values for length.

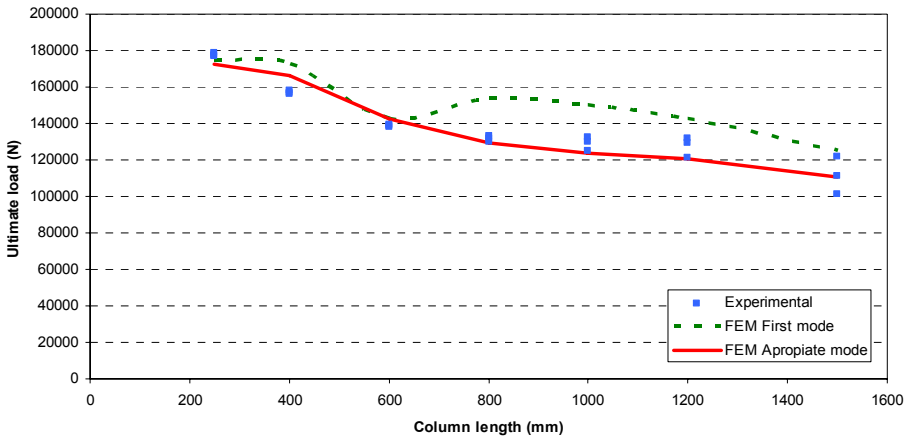

Figure 14: Comparison of conventional FEM models with experimental results

There is a good agreement between the (appropriate mode) method and experimental results. On the other hand the (first mode) method provides no reliable results.

4.3 Residual stresses included in the finite element model

In this Section results obtained by nonlinear finite element analysis including residual stresses are compared with the experimental tests, and also with the standard approach presented in Section 4.2. Solid 186 (20-node element) has been used in this case.

The nonlinear analysis is performed by including the residual stresses obtained in Section 3.3 as an initial stress state, instead of using the linear elastic buckling to obtain an initial deformation shape.

Ultimate load, or failure load, obtained by FEM including residual stresses is listed below for all tested lengths, and compared to the experimental data. Table 4 and Figure 15 reveal that predicted results are in good agreement with experiments.

Column length (mm)	Ultimate load (N)	FEM/EXP
250	169216	0.95
400	157694	1.00
600	141146	1.02
800	134419	1.02
1000	129900	1.00
1200	124880	0.97
1500	116326	1.04
	Mean	1.00
	S	0.032

Table 4: FEM results including residual stresses

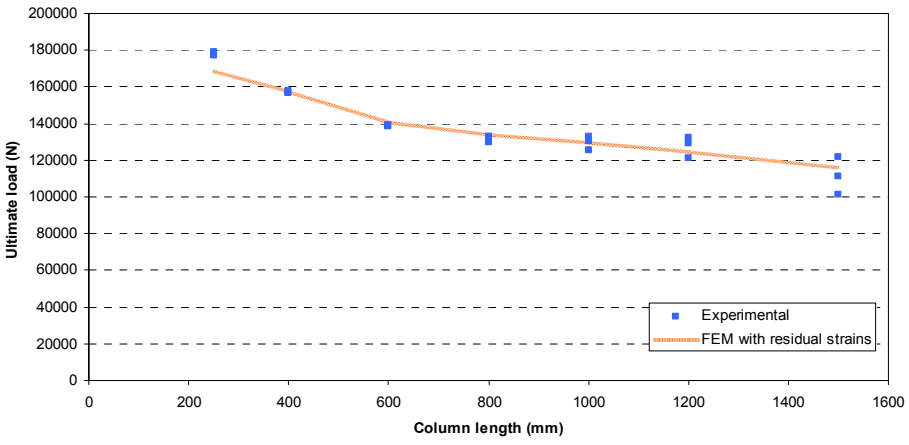

Figure 15: FEM model including residual stresses together with experimental results

Finally, Figure 16 compares the conventional (first mode) FEM model and FEM model including residual stresses with experimental results.

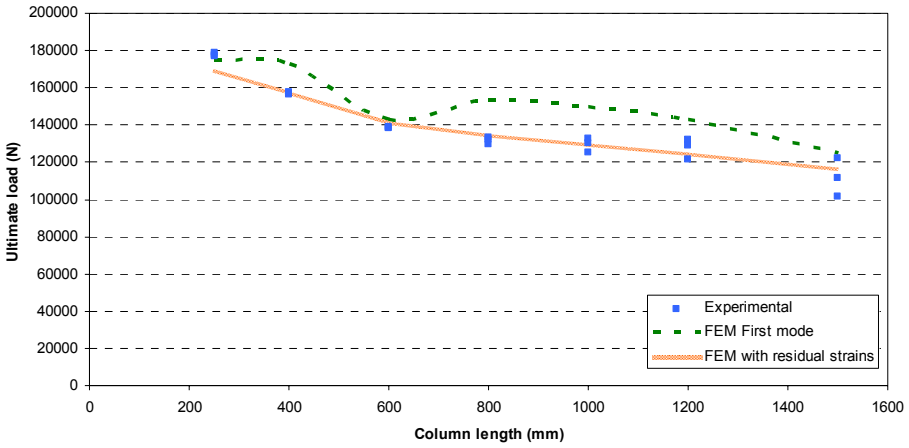

Figure 16: Comparison of conventional (first mode) FEM model and FEM model including residual stresses with experimental results

5 Conclusion

- The simulation of the cold roll forming process of the upright provides complete information about the residual strains and stresses introduced in every part of the section during the process.
- The transfer of residual strains produced in the roll forming process, as initial strains into the FE model that will be used to analyse the behaviour of the upright under compression, has been done successfully. After equilibrium, the elastic strain pattern of both models has been compared, and is very similar.
- The initial geometric imperfections generated by the residual strains in the FE model are much smaller than the conventional imperfections commonly used in the classic two step analysis method.
- It is not necessary to define an initial geometrical imperfection if residual stresses are introduced in the finite element model.
- The ultimate loads obtained by simulation with the residual strains agree very well with the experimental results (mean ratio: 1.00, deviation: 0.03). They agree better than the results obtained with the conventional two step method (mean ratio: 1.09, deviation: 0.06.

References

[1] B.W. Schafer, Z. Li, C.D. Moen, “Computational modeling of cold-formed steel”, Thin-Walled Structures, 48, 752-762, 2010.

[2] P. Borges, D. Camotim, N. Silvestre, “FEM-based analysis of the local-plate/distortional mode interaction in cold-formed steel lipped channel columns”, Computers and Structures, 85, 1461-1474, 2007.
[3] B.W. Schafer, T. Peköz, “Computational modeling of cold-formed steel: characterizing geometric imperfections and residual stresses”, Journal of Constructional Steel Research, 47, 193-210, 1998.
[4] D. Dubina, V. Ungureanu, “Effect of imperfections on numerical simulation of instability behaviour of cold-formed steel members”, Thin-Walled Structures, 40, 239-262, 2002.
[5] C.D. Moen, T. Igusa, B.W. Schafer, “Prediction of residual stresses and strains in cold-formed steel members”, Thin-Walled Structures, 46, 1274-1289, 2008.
[6] DATA M Sheet Metal Solutions GmbH. COPRA FEA RF software.
[7] ANSYS Inc. Ansys Documentation
[8] European Standard EN 1993-1-5:2006/AC:2009. Eurocode 3 – Design of steel structures - Part 1-5: Plated structural elements. European Committee for standardization, Brussels, 2009.
[9] F. Roure, M.M. Pastor, M. Casafont, M.R. Somalo, “Stub column tests for racking design. Experimental testing, FE analysis and EC3”, Thin-Walled Structures, 49, 167-184, 2011.
[10] M. Casafont, M.M. Pastor, F. Roure, T. Peköz, “An experimental investigation of distortional buckling of steel storage rack columns”, Thin-Walled Structures, 49, 933-946, 2011.